Dynamics of turbulence spreading in magnetically confined plasmas

Ö. D. Gürcan and P. H. Diamond[a)]
University of California at San Diego, La Jolla, California 92093-0319

T. S. Hahm
Princeton Plasma Physics Laboratory, Princeton, New Jersey 08543-0451

Z. Lin
University of California at Irvine, Irvine, California 92697-4575

(Received 26 August 2004; accepted 30 November 2004; published online 14 February 2005)

A dynamical theory of turbulence spreading and nonlocal interaction phenomena is presented. The basic model is derived using Fokker–Planck theory, and supported by wave-kinetic and K-ϵ type closures. In the absence of local growth, the model predicts subdiffusive spreading of turbulence. With local growth and saturation via nonlinear damping, ballistic propagation of turbulence intensity fronts is possible. The time asymptotic front speed is set by the geometric mean of local growth and turbulent diffusion. The leading edge of the front progresses as the turbulence comes to local saturation. Studies indicate that turbulence can jump gaps in the local growth rate profile and can penetrate locally marginal or stable regions. In particular, significant fluctuation energy from a turbulent edge can easily spread into the marginally stable core, thus creating an intermediate zone of strong turbulence. This suggests that the traditional distinction between core and edge should be reconsidered. © *2005 American Institute of Physics*. [DOI: 10.1063/1.1853385]

I. INTRODUCTION

One of the most formidable obstacles to achieving high performance of magnetically confined plasmas, sufficient for controlled fusion, is the development of the capability to predict and control the turbulent transport of heat, particles, momentum, etc. In recent years, progress in experiment, theory, and computation has been dramatic, yet the "Holy Grail" of predictive capacity by other than brute force, case-by-case direct numerical simulation, remains elusive. Several of the remaining challenges may be loosely characterized as related to *mesoscale phenomena*, a category which refers to dynamics on scales larger than a mode or integral scale eddy size, but smaller than the system size or profile scale length.[1,2] Transport barriers,[3,4] avalanches,[5] and heat and particle pulses are all mesoscale phenomena. Propagating transport barriers couple a turbulence quenching "front" to the buildup of steep pressure gradients, strong velocity shears, etc. Avalanches and pulses are due to strong, local excitation of turbulence causing a spillover of the profile gradient into a neighboring region, thus triggering more strong turbulence and transport, etc., rather like the toppling of an array of dominos. Experience has shown such mesoscale dynamics to be extraordinarily difficult to realize in direct numerical simulations, on account of the breakdown of the disparity between turbulence and transport time scales. This suggests that a simpler approach to modeling and describing mesoscale dynamics may be productive.

Nearly all mesoscale phenomena involve, to some extent, the spatial propagation of turbulence or its direct inverse process, namely, the propagation and broadening of transport barriers. In the case of transport barrier formation, turbulence actually retreats, rather than spreads, but the dynamics of these processes are quite similar. Examples of turbulence spreading at the back transition include Refs. 6,7. Certainly the retreat of a barrier, as at the back transition, is a classic case of "turbulence spreading."[8] Avalanches involve turbulence spreading mediated by local gradient steepening and relaxation. It is easy to see that the spatial propagation of a turbulent region or patch is a common element of all these phenomena. This is an especially pertinent observation, since it is equally true that virtually all models of fluctuation levels and turbulent transport are built on an assumption of *local balance* of linear growth with linear damping and nonlinear coupling to dissipation.[9] Here, "local balance" refers to balance at a point or in a region comparable in extent to the modal width. Such models thus necessarily exclude mesoscale dynamics. Even when bifurcation transitions are modeled, they usually are treated locally, leaving the question of barrier *width* largely unaddressed.

It is certainly appropriate, then, to identify mesoscale dynamics as an important category of poorly understood phenomena. In such an instance, it is usually helpful to identify and study in depth the simplest, most minimal problem in the genre before proceeding to consider more complicated examples. In this case, the "minimal problem" is that of the spatiotemporal propagation of a patch of turbulence from a region where it is locally excited to a region of weaker excitation, or even local damping. Understanding the simple problem is, as we shall see, crucial to the construction and interpretation of numerical simulations of microturbulence, as well as to understanding the physical phenomena. The phenomenon of spreading or propagation of turbulence has been the subject of attention in the research community for some time.[10,11] Describing the development of a turbulent burst, such as that which occurs at vortex tube reconnection,

[a)]Also at Isaac Newton Institute, University of Cambridge, United Kingdom.

is a classic problem in fluid dynamics. Turbulence spreading was first studied systematically in the context of fusion plasmas by Garbet *et al.*,[12] who sought to understand and explain nonlocal relaxation phenomena. This study compared linear (associated with toroidicity) and nonlinear spatial energy transfer processes. Subsequently, spreading phenomena have been observed in several computer simulations.[13,14] In the past two years, there has been renewed interest in spreading on account of the hypothesis that it may be related to the breakdown of gyro-Bohm scaling observed in numerical simulations.[15–17] A simple theoretical model was proposed to support this hypothesis.[18,19] Later, zonal flow coupling in toroidal geometry was suggested as an alternative means of facilitating spreading.[20]

Previously, the spreading process was described by a single phenomenological equation for the local turbulence intensity ε, which includes the effects of local linear growth and damping, spatially local nonlinear coupling to dissipation and spatial scattering of turbulence energy induced by nonlinear coupling.[15,19] These effects combine to give an energy equation (loosely) of the form

$$\frac{\partial \varepsilon}{\partial t} - \frac{\partial}{\partial x} D(\varepsilon) \frac{\partial \varepsilon}{\partial x} = \gamma(x)\varepsilon - \gamma_{\mathrm{NL}}(x)\varepsilon(x)^2,$$

the terms of which correspond to nonlinear spatial scattering [i.e., typically $D(\varepsilon) \sim \varepsilon$], linear growth and damping, and local nonlinear decay, respectively. Here $\gamma_{\mathrm{NL}}(x)$ is a spatially varying coupling coefficient. The local nonlinear damping term captures the effect of saturation via coupling to smaller scales due to local mixing. The local saturation level $\varepsilon(x) = \gamma(x)/\gamma_{\mathrm{NL}}(x)$ then corresponds to the traditional and time honored "mixing length" level. This energy equation is the irreducible minimum of the model, to which additional equations for other fields, and contributions to dynamics which feedback on ε may be added. Note that the above energy equation manifests the crucial effect of spatial coupling in the nonlinear diffusion term. The latter arises as a natural consequence of nonlinear coupling in an inhomogeneous system, i.e.,

$$(\underline{k} \cdot \underline{k}' \times \underline{z})^2 |\tilde{\phi}_{\underline{k}'}|^2 \tau_{c\underline{k}'} \varepsilon_k \rightarrow - \frac{\partial}{\partial x} D \frac{\partial}{\partial x} \varepsilon_k + k_\theta^2 D \varepsilon_k,$$

where

$$D = \sum_{\underline{k}'} |\tilde{V}_{r_{\underline{k}'}}|^2 \tau_{c\underline{k}'}.$$

Coupling in $\underline{k}$ and scattering in space are inexorably coupled. In particular variation in the spatial envelope of turbulence will result in intensity profile readjustment. The energy equation implies that the integrated fluctuation intensity in a region of extent Δ about a point x [i.e., $\int_{x-\Delta}^{x+\Delta} \varepsilon(x')dx'$] can grow, *even for negative* $\gamma(x)$, so long as $D(\varepsilon)\partial\varepsilon/\partial x|_{x-\Delta}^{x+\Delta}$ is *sufficiently large.* Alternatively, ε can decrease, *even for positive* $\gamma(x)$, should $D(\varepsilon)\partial\varepsilon/\partial x|_{x-\Delta}^{x+\Delta}$ be *sufficiently negative.* Note that sgn $[D(\varepsilon)\partial\varepsilon/\partial x|_{x-\Delta}^{x+\Delta}]$ thus defines a simple nonlocal criterion, in terms of the fluctuation intensity profile, for the influx or outflow of turbulent energy from a given interval in radius. These simple observations nicely illustrate the failure of the local saturation paradigm, and strongly support the argument that propagation of turbulence energy is a crucial, fundamental problem in understanding confinement scalings for fusion devices in which growth and damping rate profiles vary rapidly in space. We also demonstrate that the combined effects of local growth and nonlinear diffusion leads to a propagating fluctuation front. Such a solution exists for finite, local nonlinear saturation, and will appear as a ballistically expanding front, with speed $v \sim (\gamma D)^{1/2}$, where $D = D_0 \gamma/\gamma_{\mathrm{NL}}$.

Another aspect of the dynamics which falls outside the traditional "local balance" paradigm of the ground-breaking monograph by Kadomtsev is illustrated by the equation for $\varepsilon(x)$. First, turbulence energy propagation is intrinsically nondiffusive, since $D(\varepsilon)$ increases with ε. This is easily seen by observing that for $D(\varepsilon) = D_0\varepsilon$, the natural diffusive scalings for the width of a turbulent patch are $\ell^2 \sim D_0 \varepsilon t$ and $\varepsilon\ell \sim E_0 = \varepsilon_0 \ell_0$. It thus follows that the self-similarity variable is $x/\ell(t) = x/(D_0 E_0 t)^{1/3}$, so a turbulent patch spreads as $\Delta x \sim (D_0 E_0 t)^{1/3}$ in the absence of growth or dissipation. Contrary to naive expectations, this actually corresponds to *subdiffusive* propagation, which has the property of accelerated progression at small t, followed by slower progression at late times. In this paper, we show that a localized pulse in a nonlinearly saturated linearly unstable region spreads ballistically with velocity given by $v^2 = \gamma^2 D_0/2\gamma_{\mathrm{NL}}$. These analyses also underscore the importance of boundary conditions, stability profiles, and gradient control in determining the outcome of numerical simulations. Thus, the rapid readjustment and spatial spreading of turbulence intensity profiles observed in several gyrokinetic particle simulations are quite likely symptoms of turbulence propagation. Although it is a fact that the numerical simulations capture the locally saturated state rather accurately, it is not clear that they run for sufficient time to reveal the full effects of turbulence spreading and the secondary saturation that is sometimes reached when the spillover of turbulence is balanced by the damping rate in the numerical "buffer zone."[21] It is important that these simulations be properly constructed so as to "contain" turbulence spreading, while avoiding unphysical backscatter, boundary reflection, etc., of propagating turbulence fronts, such as those discussed earlier.

The purpose of this paper is to discuss the *foundations* of the theory of turbulence spreading and propagation. We demonstrate that an equation for the mean fluctuation energy density, with the structure given above, can be obtained by either a Fokker–Planck analysis of the energy density evolution or by the application of quasilinear theory to the wave kinetic equation. The spatial evolution equation for ε obtained in each case is (not surprisingly) the same. Physically motivated arguments (based on considerations familiar from $K-\epsilon$ modeling) for the form of the nonlinear diffusion term are supplied as well. The crux of these arguments is that in an inhomogeneous medium, spatial scattering and spreading are necessarily coupled to spectral transfer to small scale. Thus, the turbulence spreading phenomena is seen to be generic. Notice that this model is inherently different from that in Ref. 22 in an essential way, in that it describes the evolution of the fluctuation "wave action" rather than its deviation

from the SOC value. This is important, since the symmetry arguments of those models do not apply to this one.

Indeed, the model presented here has many similarities to $K-\epsilon$ models, familiar in the context of fluid turbulence. We consider various cases, depending on the local growth and damping profile $\gamma(x)$, the (initial) fluctuation profile, as parametrized by $\Delta' = (1/\varepsilon)D(\varepsilon)\partial\varepsilon/\partial x)|_{x^-}^{x^+}$, where $[x_-, x_+]$ denotes the spatial interval of interest. In particular, we are especially concerned with the dynamics and extent of propagation driven by a strongly localized source and with determining the depth of propagation into a locally stable region. As a simple, basic example, we demonstrate that the similarity solution for an initially localized slug of turbulence, which expands in a medium with constants γ, γ_{NL}, and D_0, exhibits a front solution propagating at constant speed. This result suggests that local saturation models, such as $D = \gamma/k_\perp^2$, miss an important element of the dynamics. They also suggest that toroidicity and zonal flow effects are not necessary to realize ballistic spreading. Indeed, ballistic spreading has also been shown to occur in a related system with *subcritical* excitation. A variety of $\gamma(x)$ profiles for the unstable $\rightarrow$ damped transition region (i.e., gradual, abrupt, etc.) are examined. We also consider the time required for turbulence to "tunnel" through a stable region of finite extent. Our predictions are discussed in light of, and compared to, results from recent gyrokinetic particle simulations.

The remainder of this paper is organized as follows. In Sec. II, a Fokker–Planck theory of turbulence spreading is presented and discussed. The local, nonlinear drift-diffusion equation for turbulence intensity is presented and discussed. A derivation of the intensity equation based on wave kinetics is also presented. Toroidicity effects are modeled by a radial group velocity in the outboard direction, with a magnitude set by the curvature drift velocity. Section III presents studies of the dynamics of turbulence spreading. We derive a similarity solution of the nonlinear energy equation for the case of constant coefficients. The time asymptotic solution is one of spreading at constant velocity. Propagation in various profiles of $\gamma(x)$ is examined, as well. Section IV contains a discussion and conclusions.

II. FOKKER–PLANCK THEORY OF TURBULENCE SPREADING

In this section, we present a Fokker–Planck[23] model of turbulence intensity spreading and propagation. The aim here is to derive a simple theoretical model of spatiotemporal intensity evolution and to understand the physics underpinning such a model. We proceed very much in the spirit of a $K-\epsilon$ model of turbulence by deriving a nonlinear evolution equation for $\varepsilon(x,t)$, the local (in radius) turbulence intensity. $K-\epsilon$ models have been used to study both fluid and plasma turbulence. The dynamics of $\varepsilon(x,t)$ include local growth and local nonlinear dissipation, as well as nonlocal couplings, represented by an integral operator incorporating a transition probability (Ref. 24, or see Ref. 25 for a recent review) for spatial steps, or spreading. We first proceed via Fokker–Planck theory and thus derive a nonlinear diffusion equation for $\varepsilon(x,t)$. The structure of this equation can be understood in light of the fundamental nonlinear couplings of the primitive equations.

The basic components of a Fokker–Planck theory of turbulence intensity propagation are $\varepsilon(x,t)$, the local turbulence energy density, and $T(x,\Delta x,\Delta t)$, the transition probability for a "step" of the intensity $\varepsilon(x,t)$ of size Δx in time interval Δt. Here the steps correspond to random radial couplings on mesoscales, i.e., spatial scales in excess of the mode correlation length and times longer than the local correlation time (i.e., $\Delta x > \Delta x_c$ and $\Delta t > \tau_c$). Thus, spreading is ultimately tied to the inherent fluctuations in, or unpredictability of, integral scale (i.e., mixing length scale) eddies or modes. Here, $\varepsilon(x,t)$ refers to the intensity at r, integrated over θ, ϕ. Of course, conservation of probability requires

$$\int d(\Delta x) T(x,\Delta x,\Delta t) = 1, \tag{1}$$

so the transition probability must be normalizable. Furthermore, $\gamma(x)$ here is the local excitation or growth rate, while $\gamma_{\mathrm{NL}}(x)$ represents the local nonlinear damping rate, representative of local nonlinear transfer to dissipation. Thus,

$$\gamma_{\mathrm{NL}}(x) = \gamma_{\mathrm{NL}}\varepsilon^{\alpha}, \tag{2}$$

where γ_{NL} is a coefficient and $1/2 < \alpha < 1$. Typically, $\alpha \sim 1$ for weak turbulence, and $\alpha \sim 1/2$ for strong turbulence, on account of the amplitude dependence of the correlation time. Thus, $\varepsilon(x,t)$ evolves according to

$$\varepsilon(x,t+\Delta t) = \varepsilon(x,t) + [\gamma(x)\varepsilon(x) - \gamma_{\mathrm{NL}}\varepsilon^{\alpha+1}(x)] + \int d(\Delta x) T(x,\Delta x,\Delta t)\varepsilon(x-\Delta x,t). \tag{3}$$

Note that the first term (in brackets) corresponds to *radially local* growth and decay, while the second corresponds to spatial propagation. Of course a Fokker–Planck argument assumes Markovian evolution *ab initio*. The justification for this is that we are concerned with the fluctuation intensity envelope, which is slowly varying in space and time in comparison to the fluctuations themselves, i.e., $\partial_t\varepsilon \ll \omega\varepsilon$ and $\partial_X\varepsilon \ll k\varepsilon$. The fluctuations themselves determine the step sizes and times. We also neglect flow interaction and evolution, and assume that the second moment of the local transition probability is convergent. Violation of the latter would necessitate a treatment of ε evolution via fractional kinetics.

Now, we proceed by assuming $\Delta x\varepsilon'/\varepsilon < 1$, so that an expansion of the interaction kernel is possible. The validity of this approximation requires that the step size Δx be smaller than the gradient scale of the fluctuation intensity. This approximation may fail at the edge, at the boundary of transport barriers and in other regions with steep gradients, in which case Eq. (3) becomes

$$\varepsilon(x,t)+\Delta t\frac{\partial\varepsilon}{\partial t}=[\gamma(x)-\gamma_{NL}\varepsilon^{\alpha}]\varepsilon\Delta t + \int d(\Delta x)T(x,\Delta x,\Delta t)\varepsilon(x,t) - \frac{\partial}{\partial x}\left[\int d(\Delta x)T(x,\Delta x,\Delta t)\Delta x\varepsilon(x,t)\right] + \frac{1}{2}\frac{\partial^2}{\partial x^2}\left[\left(\int d(\Delta x)T(x,\Delta x,\Delta t)\Delta x\Delta x\right)\times\varepsilon(x,t)\right]. \tag{4}$$

Now, noting the normalizability of T and rewriting the integrals over T yields

$$\int d(\Delta x)T=1, \tag{5a}$$

$$\int d(\Delta x)T\Delta x=\langle\Delta x\rangle, \tag{5b}$$

$$\int d(\Delta x)T(\Delta x)^2=\langle\Delta x\Delta x\rangle. \tag{5c}$$

Thus, the intensity evolution equation then follows as

$$\frac{\partial}{\partial t}\varepsilon(x,t)=[\gamma(x)-\gamma_{NL}\varepsilon^{\alpha}]\varepsilon(x,t)-\frac{\partial}{\partial x}[V_{\varepsilon}\varepsilon(x,t)] + \frac{\partial^2}{\partial x^2}[D_{\varepsilon}(\varepsilon)\varepsilon(x,t)], \tag{6a}$$

where

$$V_{\varepsilon}=\langle\Delta x/\Delta t\rangle \tag{6b}$$

is the intensity drift velocity and

$$D_{\varepsilon}\langle\Delta x\Delta x/2\Delta t\rangle \tag{6c}$$

is the intensity diffusivity. Note that both V_{ε} and D_{ε} are fluctuation intensity dependents.

Equation (6a) is a Fokker–Planck equation for the coarse-grained (on scale of Δ_c) turbulence energy density. The key unresolved issue is, of course, how to calculate the drift and diffusion V_{ε} and D_{ε}, a challenge which, in turn, requires us to face up to the underlying physics of radial propagation of turbulence energy. We argue by correspondence with the familiar wave kinetic equation

$$\frac{\partial N}{\partial t}+(v_{gr}+v)\cdot\nabla N-\frac{\partial}{\partial x}(\omega+k\cdot v)\cdot\frac{\partial N}{\partial k}=\gamma_{\mathrm{NC}}N, \tag{7}$$

which states that the wave population density (which usually, but not always, corresponds to the wave action density) is conserved along ray trajectories given by

$$\frac{dx}{dt}=v_g+v, \tag{8a}$$

$$\frac{dk}{dt}=\frac{-\partial}{\partial x}(\omega+k\cdot v), \tag{8b}$$

up to nonpopulation density conserving processes, represented by $\gamma_{\mathrm{NC}}N$, on the right-hand side (RHS) of Eq. (7). Note that integrating Eq. (7) over k yields an evolution equation for a local wave density. Thus, by correspondence with Eq. (8a), in which $v(x,t)$ is a local flow velocity on scales large and/or slow as compared to those of the underlying waves, and v_g is the wave group velocity, we can write

$$\frac{dx}{dt}=v_{gr}+\langle v_r\rangle+\delta v_r. \tag{9a}$$

Here v_{gr} is the radial group velocity of the fluctuations, $\langle v_r\rangle$ is the mean radial wave energy flow, and δv_r is the fluctuating large-scale flow, which induces mesoscale random radial couplings and the resulting random walk of turbulence energy density. Physically, δv_r is associated with the spatial variability of the integral scale fluctuations, and thus must be determined by their space-time scales. Application of standard methods from the theory of random processes gives

$$\frac{d}{dt}\delta x=\delta v_r, \tag{9b}$$

$$D=\int_{\infty}^{0}d\tau\langle\delta v_r(0)\delta v_r(\tau)\rangle\cong D_0\varepsilon^{\alpha}. \tag{9c}$$

This variability is inexorably coupled to the mixing process which underlies the general concept of the mixing length. The dynamics responsible for each is nonlinear coupling.

Clearly some further explanation of space and time scales is in order. Here, $\langle v_r\rangle$ refers to a mean radial flow, coherent and large scale as compared to both the underlying turbulence and waves, and the processes responsible for the propagation of turbulence. Crudely put, $\langle v_r\rangle$ may be thought of as a quasicoherent convective cell, or a "streamer" flow field.

δv_r then is due to fluctuations in this flow field, on account of nondeterministic behavior in the radial convection velocity. Thus, δv_r corresponds to fluctuations in the radial flow induced by integral scale eddies and waves. Note that the model thus involves *four scales*, namely, Δx_c (the correlation length of the basic turbulence), $\delta\ell$ (the length scale for random walk of turbulence intensity), $\Delta\ell$ (the length scale of quasicoherent convective cells), and the macroscopic scale lengths associated with gradients and the system size. In practical terms, $\delta\ell$ is set by the turbulence mixing length scale. Again, we see that the concepts of turbulence spreading and turbulent mixing are quite closely related, and both stem from the same characteristic scale of turbulent motion. We caution the reader here that the mixing length does not at all necessarily correspond to the linear mode width, as is usually assumed.

The fluctuations δv_r on scales $\delta\ell$ correspond to fluctuations in radial flow rates induced by large incoherent eddies. These motions may be thought of as somewhat related to "avalanches," except that here we are concerned with trans-

port of fluctuation intensity, not heat, particles, etc. Nevertheless, the obvious synergism between gradient drive and fluctuation level strongly suggests that these two phenomena are related, and that intensity bursts are possible. Thus, an inclusive model of turbulence propagation should treat the evolution of profiles and the electric field, as well as $\varepsilon(x,t)$. Indeed, simple forms of such an archetypical model have already been constructed and used to describe transport barrier dynamics (which may be thought of as the spreading of "antiturbulence"). Here, however we focus on self-scattering and self-spreading of turbulence alone, and thus do not attempt to present a complete model including profile evolution. It is, however, important to stress that the statistical structure of the transition probability need *not* be Gaussian. Indeed, studies of avalanches lead us to expect that T is likely quasi-Gaussian for moderate Δx, with a non-Gaussian tail for large Δx. The latter may indeed be a power law, which in turn could render the second moments [as given in Eqs. (6b) and (6c)] of T undefined. In such a case, the turbulence propagation will be strongly bursty and intermittent, and must be described via a fractional kinetics approach.[26]

Proceeding with the calculation, we hereafter assume (for simplicity) that no large-scale coherent flow is present, and thus ignore $\langle v_r \rangle$. We shall later consider a simple model that includes the radial mean intensity flux driven by fluctuation-fluctuation coupling. Such a model has different characteristics, since the nonlinear diffusion of $\varepsilon(x,t)$ occurs via its advection by the mean radial flow similar to the advection of a passive scalar.

Thus neglecting $\langle v_r \rangle$, V_ε and D_ϵ may be written as

$$V_\varepsilon = v_{gr}(x) + \hat{V}_\varepsilon, \tag{10a}$$

$$D_\varepsilon = D_{0,\alpha}\varepsilon^\alpha. \tag{10b}$$

Here, as before, $\alpha=1$ for weak turbulence and $\alpha=1/2$ for strong turbulence, where $D_{0,\alpha}$ gives the relevant scaling of the diffusion coefficient for fluctuation intensity, which in practice is set by the scaling of the nonlinear couplings at large scales. Following the Stratonovich calculus[27] interpretation of the Fokker–Planck theory, $V_{\varepsilon,\alpha}$ corresponds to that piece of the drift, which is associated with the spatial gradient of D_ε, i.e.,

$$\hat{V}_\varepsilon = \frac{\partial}{\partial x}(D_{0,\alpha}\varepsilon^\alpha). \tag{11a}$$

Thus, nonlinearity and fluctuation profile structure produce a mean turbulence energy drift, as well as a diffusion. The equation for $\varepsilon(x,t)$ can then be written as

$$\frac{\partial}{\partial t}\varepsilon + \frac{\partial}{\partial x}[(v_g\varepsilon)] - \frac{\partial}{\partial x}D_{0,\alpha}\varepsilon^\alpha\frac{\partial\varepsilon}{\partial x} = [\gamma(x) - \gamma_{\mathrm{NL}}\varepsilon^\alpha]\varepsilon. \tag{11b}$$

Equation (11b) is the working equation for $\varepsilon(x,t)$ which is the primary focus of our attention hereafter. The various terms in Eq. (11b) correspond to linear propagation of energy by waves, spatial flow of energy induced by fluctuation intensity gradient, spatial diffusion of energy by random nonlinear couplings, and local linear growth and nonlinear decay, respectively. Equation (11b) represents a hybrid of a wave kinetic equation and a $K-\epsilon$ model equation for turbulence, as a consequence of its mixture of linear and nonlinear effects. Note also that the diffusion here is nonlinear, since $D\sim\varepsilon^\alpha$. The space-time dynamics of the turbulence intensity are described by Eq. (11b), which can be recast in conservative form as

$$\frac{\partial\varepsilon}{\partial t} + \frac{\partial}{\partial x}\Gamma_\varepsilon = S_\varepsilon. \tag{12a}$$

Here,

$$\Gamma_\varepsilon = (v_{gr}\varepsilon) - (D_{0,\alpha}\varepsilon^\alpha)\frac{\partial\varepsilon}{\partial x} \tag{12b}$$

is the intensity flux and

$$S_\varepsilon = [\gamma(x) - \gamma_{\mathrm{NL}}\varepsilon^\alpha]\varepsilon \tag{12c}$$

is the local source and sink. The intensity flux contains deterministic drifts (proportional to v_{gr}) and a nonlinear Fickian diffusion term $(D_{0,\alpha}\varepsilon^\alpha)\partial\varepsilon/\partial x$, the latter implying that turbulence intensity gradients drive a diffusive flux of fluctuation energy. Nonlinear interaction and coupling enter in two ways, namely, as a local sink on the RHS, which represents local transfer to dissipation, and as spatial coupling effects on the LHS. This reflects the fact that the nonlinearity scatters fluctuation energy both spatially and in wave number space.

Equation (12a) also gives a simple relation for the time rate of change of fluctuation energy in the finite interval $[x_-,x_+]$. Integrating Eq. (12a) straightforwardly yields

$$\frac{\partial E}{\partial t} = -\Gamma_\varepsilon\Big|_{x_-}^{x_+} + S, \tag{13}$$

where $\Gamma_\varepsilon|_{x_-}^{x_+}$ is the net flux in/out of the region and S is the integrated sink term. Thus, $\partial E/\partial t>0$ is possible if either $\Gamma_\varepsilon|_{x_-}^{x_+}>0$ or $S>0$, so that a linearly stable region can support fluctuations which are excited elsewhere and couple into it. Even if $S<0$, a sufficiently large $\Gamma_\varepsilon|_{x_-}^{x_+}$ is sufficient for local growth. It is also interesting to observe that

$$\Gamma_\varepsilon\Big|_{x_-}^{x_+} = v_{gr}\varepsilon\Big|_{x_-}^{x_+} + \Delta'_\varepsilon\varepsilon, \tag{14a}$$

where

$$\Delta'_\varepsilon\varepsilon = \frac{\partial}{\partial x}\frac{D_{0,\alpha}\varepsilon^{1+\alpha}}{1+\alpha}\Bigg|_{x_-}^{x_+}. \tag{14b}$$

In the absence of local sources or radial wave propagation, we see that $\partial E/\partial t>0$ requires $\Delta'_\varepsilon\varepsilon>0$, which defines a condition on the fluctuation intensity profile for local growth. Obviously $\Delta'_\varepsilon\varepsilon>0$ implies a net *influx* of turbulence to the region $[x_-,x_+]$, while $\Delta'_\varepsilon\varepsilon<0$ implies an outflow. As is obvious, should $\Delta'_\varepsilon\varepsilon$ be sufficiently large, growth in the region can occur even if $\gamma<0$.

It is also illuminating to amplify and extend the discussion of the relationship between turbulence spreading and mixing length theory. For simplicity, consider simple shear-driven, incompressible Navier–Stokes turbulence. In that

case [for $\underline{V}=V(x)\hat{z}+\tilde{\underline{V}}$], the mean intensity flux $V(x)$ evolves according to the Reynolds averaged equation

$$\frac{\partial}{\partial t}\langle V(x)\rangle = -\frac{\partial}{\partial x}\langle \tilde{V}_x\tilde{V}_z\rangle + \nu\frac{\partial^2\langle V\rangle}{\partial x^2}, \tag{15a}$$

while the average turbulence kinetic energy evolution is governed by

$$\frac{\partial}{\partial t}\langle \varepsilon(x,t)\rangle + \frac{\partial}{\partial x}\langle \tilde{V}_x\varepsilon\rangle = -\langle \tilde{V}_x\tilde{V}_z\rangle\frac{\partial}{\partial x}\langle V_z\rangle - \frac{\partial}{\partial x}\langle \tilde{V}_x\tilde{P}\rangle - \nu\langle|\boldsymbol{\nabla}\underline{V}|^2\rangle. \tag{15b}$$

Here, $\varepsilon=|\tilde{V}|^2/2$, $\rho=1$ for convenience, and symmetry in y,z is assumed. Equation (15b) states that the mean flow evolves via Reynolds stress-induced momentum transport and viscous dissipation, while Eq. (15b) balances fluctuation energy input by Reynolds work and pressure work, with energy transport and viscous dissipation. For incompressible turbulence, the pressure work is negligible and the $\langle\tilde{V}_x\tilde{p}\rangle$ term is hereafter neglected. This system of simple averaged equations may be closed by invoking the mixing length hypothesis, which relates fluctuations to "mixing" of averaged quantities over a scale ℓ, called the mixing length.[28] In the mixing length ansatz, the fluctuation axial flow $\tilde{V}_z$ is given by

$$\tilde{V}_z \cong -\ell\frac{\partial\langle V\rangle}{\partial x}, \tag{16a}$$

and the energy density fluctuation by

$$\tilde{\varepsilon} \cong -\ell\frac{\partial\langle\varepsilon\rangle}{\partial x}. \tag{16b}$$

Note that Eq. (16a) may be rewritten as $|\tilde{V}_z/\langle V\rangle|\sim\ell/L_v$, where $L_v^{-1}=|(1/\langle V\rangle)\partial\langle V\rangle/\partial x|$, which has the traditional form of a mixing length rule. For flow in pipes or jets, the mixing length ℓ is usually associated with some macroscopic scale, such as the distance from the wall, etc. In plasma confinement guesstimates, ℓ is usually related to a linear mode width or (preferably) a radial correlation length.

Equations (15a) and (15b) then can be reexpressed as

$$\frac{\partial}{\partial t}\langle V\rangle = \frac{\partial}{\partial x}\nu_T\frac{\partial\langle V\rangle}{\partial x} + \nu\frac{\partial^2}{\partial x^2}\langle V\rangle \tag{17a}$$

and

$$\frac{\partial}{\partial t}\langle\varepsilon\rangle - \frac{\partial}{\partial x}\nu_T\frac{\partial\langle\varepsilon\rangle}{\partial x} = \nu_T\left(\frac{\partial\langle V\rangle}{\partial x}\right)^2 - \nu\langle(\boldsymbol{\nabla}\tilde{V})^2\rangle. \tag{17b}$$

Here, the turbulent viscosity ν_T (also called the "eddy viscosity") is given by

$$\nu_T = \langle\varepsilon\rangle^{1/2}\ell. \tag{17c}$$

Equation (17b) states that fluctuation energy spreads diffusively at the same rate at which the mean flow relaxes. This simple exercise suggests that just as turbulent transport mixes mean quantities during relaxation, it also mixes and transports *fluctuation energy*. Thus, turbulent spreading goes hand-in-glove with mixing dynamics and mixing length models of turbulence. Note also that this analysis pinpoints the fundamentally nonlinear dynamics of spreading, since this phenomenon emerges directly from a consideration of the triple moment.

Wave kinetics yields yet another alternative and useful perspective on turbulent spreading. See the Appendix for a derivation of a bivariate diffusion equation using this approach.

III. DYNAMICS OF TURBULENCE SPREADING

A. Intensity front dynamics and propagation

In this section, we examine the dynamics of turbulence spreading and propagation, as described by the energy density evolution equation

$$\frac{\partial\varepsilon}{\partial t} + v_g\frac{\partial\varepsilon}{\partial x} - \frac{\partial}{\partial x}\left(D_0\varepsilon^\alpha(x,t)\frac{\partial\varepsilon}{\partial x}\right) = \gamma(x)\varepsilon - \gamma_{\mathrm{NL}}(x)\varepsilon^{\alpha+1}, \tag{18}$$

derived by Fokker–Planck methods in the preceeding section. For the case where $\alpha=1$ (weak turbulence), $\gamma=0$, $\gamma_{\mathrm{NL}}=0$, $v_g=0$, and $D_0=$const, Eq. (18) has a well-known self-similar solution[29]

$$\varepsilon(x,t) = \frac{A}{t^{1/3}}[1-x^2/d(t)^2]\Theta(|d(t)-x|), \tag{19a}$$

where

$$d(t) = (6AD_0)^{1/2}t^{1/3}. \tag{19b}$$

This solution expressed in terms of the similarity variable $x/d(t)\sim x/t^{1/3}$, describes the self-similar subdiffusive expansion of an initially localized slug of turbulence with initial impulse $A=\int dx\varepsilon(x,0)$, where $\varepsilon(x,0)$ has compact support. Hahm *et al.*[19] considered the effects of γ and γ_{NL} on this case perturbatively, with encouraging results.

The other case is $v_{gx}=$const, $\gamma=$const, and $\gamma_{\mathrm{NL}}=0$, for which another similarity solution can be obtained, which is

$$\varepsilon(x,t) = Ae^{\gamma t}\frac{(1-(x-v_{gx}t)^2/d(t)^2)}{([e^{\gamma t}-1]/\gamma)^{1/2}}\Theta(|d(t)-(x-v_{gx}t)|) \tag{20a}$$

where now

$$d(t) = (6D_0A)^{1/2}[(e^{\gamma t}-1)/\gamma]^{1/3}. \tag{20b}$$

Notice that the effect of group velocity is easily captured by a Galilean transformation. Convective propagation toward the low-field direction may be viewed as a surrogate for spreading via toroidicity-induced coupling of poloidal harmonics. This solution does not saturate, and it spreads "exponentially" fast, due to the fact that the nonlinear damping is set to zero. Indeed, it seems clear that exponential spreading is indicative of the neglect of proper damping or saturation processes in the theory. In addition to their intrinsic physics interest, these solutions define practical benchmark cases for any numerical solution of Eq. (18). Figure 1 demonstrates the excellent agreement between numerical solutions and the analytical, self-similar solutions. The numerical solutions establish the relevance of the similarity solutions:

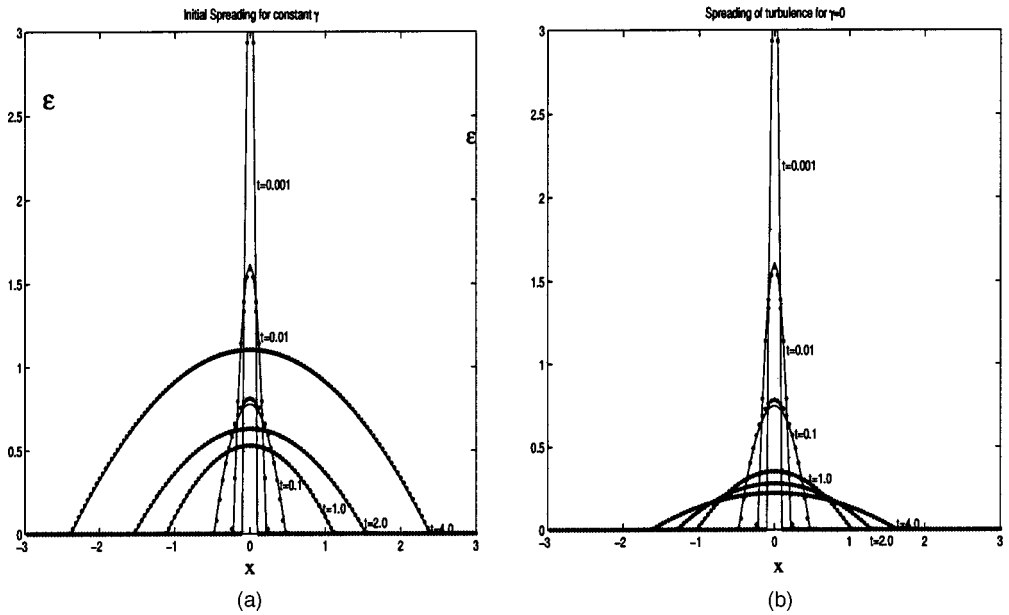

FIG. 1. Behavior of the solutions for the cases (a) $\gamma=0.5$ and (b) $\gamma=0.0$, with $\gamma_{\mathrm{NL}}=0$. The dots correspond to the result of numerical integration and the solid line corresponds to the exact analytical solution. For $\gamma=0$ the usual scaling $\xi=x/t^{1/3}$ is obtained, whereas for $\gamma=0.5$ exponential spreading is observed.

the final asymptotic forms are nearly independent of the initial conditions. Note that these are not "traditional" solutions of the diffusion equation, since the nonlinear term plays an important role in setting the diffusion rate. Another class of solutions of interest is that for the case $\gamma=\mathrm{const}$, $\gamma_{\mathrm{NL}}=\mathrm{const}$ and $D_0=\mathrm{const}$. As this case corresponds to constant or slowly varying background, it is discussed in some detail here. After the re-scalings $x\rightarrow(\gamma_{\mathrm{NL}}/2D_0)^{1/2}x, t\rightarrow\gamma t, \varepsilon\rightarrow(\gamma_{\mathrm{NL}}/\gamma)\varepsilon(x,t)$, Eq. (18) may be rewritten as

$$\frac{\partial\varepsilon}{\partial t}-\frac{1}{4}\frac{\partial^2}{\partial x^2}\varepsilon^2-\varepsilon(1-\varepsilon)=0. \tag{21}$$

Equations (20a) and (20b) are immediately recognizable as a variant of the well-known Fisher–Kolmogorov–Petrovski–Piskunov (Fisher-KPP) equation for logistic-limited epidemic propagation,[30,31] now with nonlinear diffusion. The Fisher-KPP equation is a reaction-diffusion type equation which is well known to exhibit spatiotemporally propagating front solutions.[32] A numerical solution of Eqs. (20a) and (20b) (for localized initial conditions) is shown in Fig. 2. This rather clearly suggests that the profile of $\varepsilon(x,t)$ time-asymptotically approaches an expanding front, which decays exponentially in space. This structure is similar to that of a "leading edge," which is a well-known solution of the Fisher equation. Motivated by these observations, we ansatz the similarity solution

$$\varepsilon(x,t)=f(t)(1-e^{-|x-d(t)|}-e^{-|x+d(t)|}). \tag{22}$$

Equation (22) describes a bounded, localized solution with extent $2d(t)$ and with two expanding fronts, propagating in opposite directions at speed $d(t)$, where the dot denotes differentiation with respect to time. Substituting Eq. (22) into Eq. (21) yields (for $t\rightarrow\infty$) a differential equation for $d(t)$ and an expression relating $d(t)$ to $f(t)$. These are

$$d'(t)-\frac{1}{2}+2e^{-d(t)}\frac{\cosh^{-1}(e^{d(t)}/2)}{\sqrt{-4+e^{2d(t)}}}=0 \tag{23a}$$

and

$$f(t)=\frac{1}{1-4e^{-2d(t)}}-4\frac{e^{d(t)}\cosh^{-1}(e^{d(t)}/2)}{(-4+e^{2d(t)})^{3/2}}. \tag{23b}$$

An implicit solution for $d(t)$ follows directly from Eq. (23a) in the form

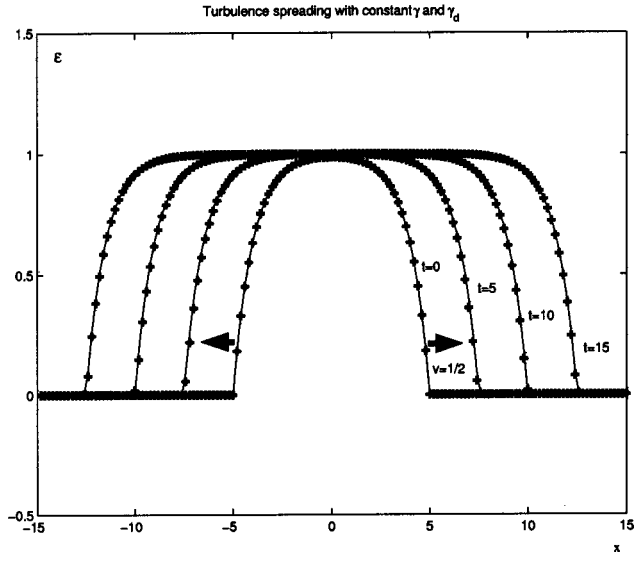

FIG. 2. Constant velocity expansion for the cases $\gamma=\mathrm{const}$ and $\gamma_{\mathrm{NL}}=\mathrm{const}$. The numerical simulation represented by the dots is in excellent agreement with the asymptotic analytical solution represented by the solid lines. Even more complex initial conditions approach the same asymptotic solution.

$$\sinh[2\cosh^{-1}(e^{d(t)}/2)] - 2\cosh^{-1}(e^{d(t)}/2) = e^t. \tag{24}$$

$d(t)$, as given by the solution of Eq. (24), defines an exact, asymptotic solution of Eq. (21) in the form suggested by Eq. (22). It is interesting to observe that for $t\to\infty$, Eq. (24) has the simple solution $d(t)=t/2$. Restoring dimensional quantities, this implies that the fluctuation energy front expands according to

$$d(t) = vt \tag{25a}$$

with a constant front velocity

$$v = \left(\frac{\gamma^2 D_0}{2\gamma_{\mathrm{NL}}}\right)^{1/2}. \tag{25b}$$

This solution suggests that the dynamics of $\varepsilon(x,t)$ developing from a localized source evolves in two steps. First, there is rapid growth to logistically limited local saturation at $\varepsilon=\gamma/\gamma_{\mathrm{NL}}$. Second, the value $\varepsilon=\gamma/\gamma_{\mathrm{NL}}$ defines an effective value of the fluctuation energy diffusion $D=D_0\varepsilon/4 = D_0\gamma/4\gamma_{\mathrm{NL}}$. The effect of the spatial coupling induced by such diffusion then combines with local growth to produce a classic Fisher-KPP front with velocity $V=(2\gamma D)^{1/2}$. Here γ is the local effective reaction (growth) rate, which corresponds in this case to turbulence growth, and D is the net effective diffusion, $D=\gamma D_0/4\gamma_{\mathrm{NL}}$. It is interesting to note that the front of turbulence energy propagates ballistically [i.e., $d(t)=vt$]. This occurs in the absence of toroidicity-induced coupling of poloidal harmonics. Thus, rapid propagation observed in turbulence simulations does not follow exclusively from linear coupling of poloidal harmonics (i.e., ballooning effects), but rather can be a more general consequence of the dynamics. Indeed, this dynamical ballistic expansion rate can easily exceed that due to toroidal coupling. Note that for standard "gyro-Bohm" scalings, $\gamma\sim v_{\mathrm{Ti}}/L_\perp$, $\gamma_{\mathrm{NL}}\sim v_{\mathrm{Ti}}/L_\perp$, and $D_0\sim\rho_i^2 v_{\mathrm{Ti}}/L_\perp$, so $v\sim\rho_i v_{\mathrm{Ti}}/L_\perp\sim V_{*i}$. In this normalization, ε is dimensionless and is scaled to the square mixing length level, so $\varepsilon\sim 1$ at local saturation. Taking v_{gx} of order of the curvature drift speed for the purposes of simulating the coupling of poloidal harmonics, $v_{gx}\sim\rho_i v_{\mathrm{Ti}}/R\sim\epsilon V_{*i}$. Thus, $v/v_{gx}\sim(1/\epsilon)$, so we find that dynamically driven expansion and spreading can progress ballistically, and in fact *faster* than geometrically induced spreading due to toroidicity. The speed of this dynamically induced ballistic spreading is set by the geometric mean of local growth (i.e., reaction rate γ) and diffusion ($D=D_0\varepsilon=D_0\gamma/\gamma_{\mathrm{NL}}$). Note also that ballistic front propagation at finite speed requires finite local nonlinear damping (i.e., $\gamma_{\mathrm{NL}}\neq 0$), so as to allow a meaningful locally saturated state. Indeed, local nonlinear damping is essential in order to accurately distinguish between nontrivial spreading phenomena and simple readjustment of an unsaturated intensity profile. The implications of neglecting nonlinear damping in Eq. (18) are further elaborated later in this paper. Whereas Eq. (22) together with Eq. (24) or Eq. (25a) is an example of ballistic spreading, the solution in Eq. (20a) is an example of exponential spreading. More generally, this simple example is a splendid illustration of the breakdown of the local saturation paradigm. In particular, this result states that though the turbulence comes to a local saturation (i.e., $\gamma=\gamma_{\mathrm{NL}}\varepsilon$), the presence of a gradient in ε (i.e., a leading edge, due to localized pulse initial conditions) forces nontrivial envelope dynamics [i.e., spreading at $v=(\gamma^2 D_0/2\gamma_{\mathrm{NL}})^{1/2}$]. These nontrivial envelope dynamics occur on time scales longer than those local fluctuations but much shorter than transport time scales, and thus are a prime example of mesoscale dynamics.

B. Intensity spillover into a stable region

We now consider the spreading of turbulence into locally marginal or damped regions from zones of linear instability.[19] To understand the radial spreading of turbulence into a linearly stable region, we should consider what happens near the boundary between stable and unstable regions. The simplest way to model such a boundary is to assume $\gamma(x)=\gamma\Theta(-x)$, where $\Theta(x)$ is the unit step function. The turbulence in the unstable region is expected to grow until a local saturation is reached, and to spread until it covers the entire unstable region. The turbulence will then start to "spill" into the stable region, leading to a steady state in the long time limit. This steady state is reached when the rate at which turbulence spills into the stable (or damped) region is equal to the damping rate of turbulence in the region. Thus, for the marginally stable case, it takes an infinite time to actually reach a steady state, which involves an infinitely large damping region with an exponentially decaying intensity profile. It is possible to estimate this steady state solution based upon local balance and the matching conditions at the boundary. The steady state profile in the $\gamma>0$ region satisfies

$$\frac{1}{4}\partial_{xx}(\varepsilon^2) + \varepsilon - \varepsilon^2 = 0. \tag{26a}$$

Multiplying by $\partial_x(\varepsilon^2)$ and integrating, we obtain

$$\varepsilon'(x) = \pm\frac{(\varepsilon(x)-1)}{\varepsilon(x)}\sqrt{\varepsilon(x)^2+\frac{2}{3}\varepsilon(x)+\frac{1}{3}}. \tag{26b}$$

It is possible to further integrate and then invert Eq. (26b) to obtain an exact solution for $\varepsilon(x)$. However, for quantifying the spillover of turbulence, only the solution in the $\gamma=0$ region is relevant. The relevant solution in this region can be written as $\varepsilon=\alpha_0 e^{-x}$. To find α_0 one should match the solution and its derivative across the discontinuity, i.e., $\alpha_0=\varepsilon_0$ and

$$\frac{\varepsilon_0-1}{\varepsilon_0}\sqrt{\varepsilon_0^2+\frac{2}{3}\varepsilon_0+\frac{1}{3}} = -\varepsilon_0, \tag{27a}$$

which yields $\alpha_0=1/2^{2/3}$. Hence, in the linearly stable region, the solution is

$$\varepsilon = \frac{\gamma}{\gamma_{\mathrm{NL}}}\left[\frac{\Theta(x)}{2^{2/3}}e^{-x/\lambda}\right], \tag{27b}$$

where $\lambda=\sqrt{(2D_0/\gamma_{\mathrm{NL}})}$ is thus the skin depth or penetration length of the turbulence. The results of a numerical study of the same problem are shown in Fig. 3. Note that the solution reached steady state in about 50–100 time units (corresponding to ω_*^{-1}) and is in good agreement with the analytical solution. It should be noted that the final turbulence profile appears to be more or less independent of the initial conditions for this equation.

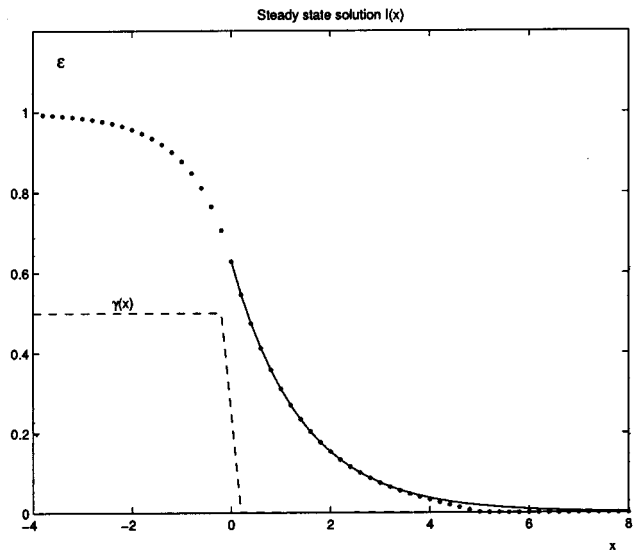

FIG. 3. Steady state solution for steplike $\gamma(x)$ profile, where $\gamma=0$ in the stable region. The dots denote the numerical integration, whereas the solid line is the analytical solution in the outer region calculated by a matching argument.

When the case of two regions, one with $\gamma>0$ and another with $\gamma<0$ (i.e., $\gamma_g=|\gamma|$, $\gamma_d=-|\gamma|$, where γ_g and γ_d are the linear growth and damping rates in the corresponding regions) is considered, a very similar picture emerges. In fact it is not difficult to find the solution for $\varepsilon(x)$ in the $\gamma<0$ region by matching the function and its derivative across the interface. The solution in that case turns out to be

$$\varepsilon = \frac{4}{3}\Theta(x)\Theta(x-x_0)\frac{|\gamma|}{\gamma_{NL}}\sinh^2\left(\frac{x-x_0}{2\lambda}\right), \tag{28a}$$

where $x_0=\lambda\cosh^{-1}(7/4)$ to match the solution in the $\gamma>0$ region. This solution is shown in Fig. 4. Thus, in the case of

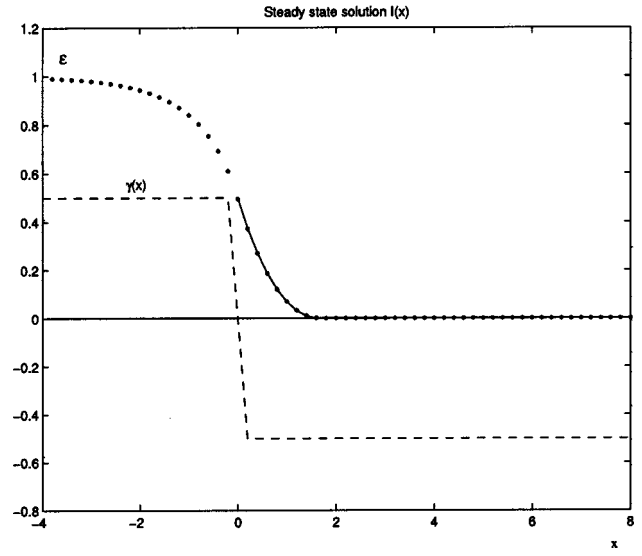

FIG. 4. Steady state solution for steplike $\gamma(x)$ profile, where $\gamma<0$ in the "stable" region. The dots denote the numerical integration, whereas the solid line is the analytical solution in the outer region calculated by a matching argument.

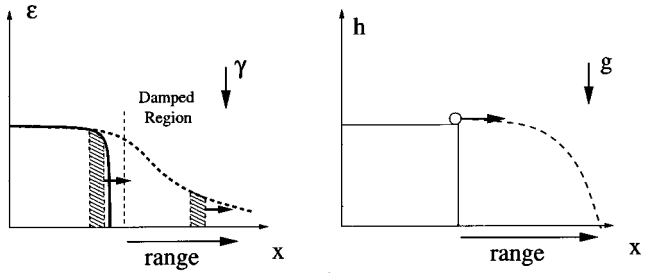

FIG. 5. Turbulence penetration depth calculated by considering eddies that are traveling with constant speed in the x direction, while being damped. An obvious analogy is with kinematics, where the height is related to ε.

a linearly damped region, the skin depth λ remains the same, but the turbulence definitely terminates at $x=x_0$, in contrast to the finding of exponential decay for the $\gamma=0$ case. When the growth rate in the unstable region γ_g and the decay rate in the decaying region γ_d are not equal in magnitude, a more general expression for x_0 can be written as

$$x_0 = \lambda\cosh^{-1}\left(\frac{3}{2}\frac{(\gamma_g/\gamma_d)}{[4(1+\gamma_g/\gamma_d)]^{1/3}}+1\right). \tag{28b}$$

Notice that x_0, which is the termination point of the turbulence region, varies mainly with γ_g/γ_d, such that for $\gamma_g \gg \gamma_d$ the turbulence penetration depth becomes large.

Another straightforward way of computing the turbulence penetration length is to consider the turbulence in the decaying region as being made up of eddies of decaying turbulence. As the eddies enter the damped region they will persist for a lifetime or a "flight time" defined as the time of decay of an eddy of initial "height" ε. It is clear that

$$t_{\text{flight}} \gtrsim 1/\gamma_d,$$

where γ_d is the decay rate. In practice, this is the time it takes for ε to e-fold in the damped region. Since the left hand side of Fig. 5 corresponds to the saturated region, in which the expansion is ballistic, with velocity given in Eq. (25b), the range of the eddy is

$$\Delta x = v t_{\text{flight}} \gtrsim \sqrt{\frac{D_0}{2\gamma_d}}.$$

This is essentially the same as λ, which was calculated by solving the steady state problem exactly in the two regions and matching these two solutions. It is remarkable that although the flight time and the velocity both change in the damped region (the expansion is not ballistic in the damped region), probably due to self-similarity, this simple argument still gives the correct answer.

Notice that although the above argument for the turbulence penetration, assumes ballistic spreading (into the stable region as well as the unstable region), it is dimensionally valid for other cases as well. This is particularly relevant for boundary control of numerical simulations, in which turbulence penetration, into a stable boundary buffer layer, can occur. The depth of this penetration in numerical simulations seems to be roughly a few ρ_*'s. However, it is not clear if this is the true "steady state" after turbulence spreading. Further study of the effects of penetration and spreading into the

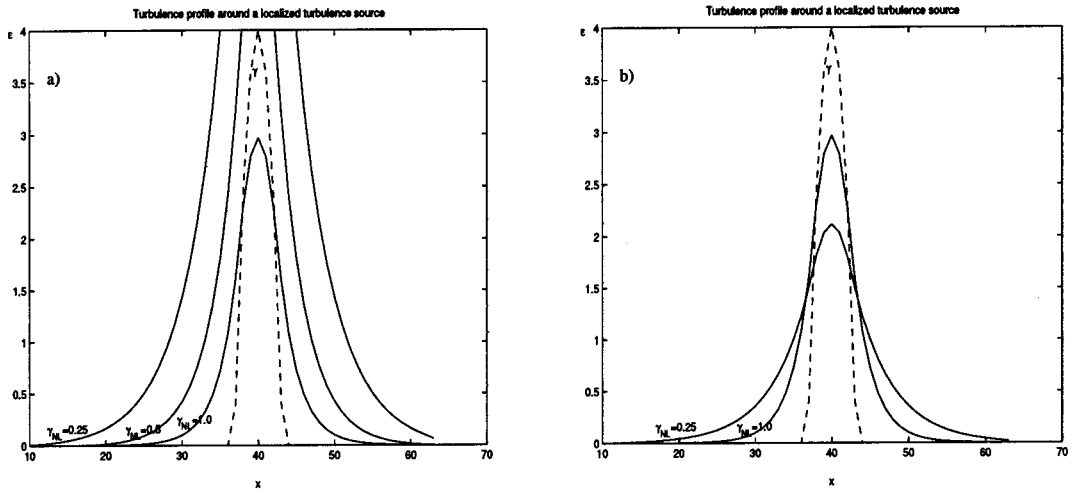

FIG. 6. Turbulence due to a strongly localized source modeling the spreading of turbulence that is produced in the edge, into the core region (a) when γ_{NL} is varied but γ is kept constant, (b) when γ_{NL} and γ are varied in such a way that $\gamma/\gamma_{\mathrm{NL}}$ is kept constant.

buffer layer of the simulation domain is clearly necessary. For instance, Eq. (28b) indicates that γ_d, which is related to the damping that is introduced near the boundary of simulation domain, should be large (i.e., larger than the growth rate in the simulation domain). If this is not the case, turbulence will penetrate more than just a few ρ_*'s into the buffer layer, and then be reflected and backscatter into the core. Moreover, this conclusion is derived from the "minimal" model, which only takes immediate fluctuations into account. More realistic models, which include a delayed response to the radial mean flux, should estimate even larger penetration. On the other hand, inclusion of zonal flow dynamics may have the opposite effect when the zonal shears are strong.

When a localized source of turbulence is considered, the spreading effect is similarly important, and therefore should be examined. According to Eq. (28b) the turbulence penetration depth is a function of γ_g/γ_d and becomes large if the damping rate is small. This suggests one particular application of the penetration idea, namely, the spreading of turbulence towards the core region when it is produced in the strongly turbulent edge, as in L mode. In this case if the damping rate [i.e., $\max(\gamma_{\mathrm{NL}},\gamma_d)$] is small, the turbulence would spread a distance of $\Delta x \gtrsim x_0$ [see Eq. (28b) for x_0] into the core. Figure 6, showing the turbulence due to a localized source, can be thought as a visualization for the spreading of turbulence, which is produced in the region of steeper gradients as in an L-mode edge, into the core region. A simple analog is that of a sprinkler. Additional dependence on γ_{NL}, the nonlinear damping rate, is shown both for fixed γ (so that as γ_{NL} decrease the local saturation level increase) and for fixed $\gamma/\gamma_{\mathrm{NL}}$. This figure also clearly shows that quite deep spreading into a quasimarginal region is possible. This effect is particularly important in hot L-mode plasmas, where the core, likely to be marginal with respect to ion temperature gradient driven modes (ITG), is adjacent to a turbulent edge. In such a case, the dynamics of spreading from the edge would produce a strongly inward turbulent transition region intermediate between the marginal core and the turbulent edge.[33] No additional instability mechanism need be invoked to explain such a region. This transition region could have significant impact on confinement predictions, as it would extend the effective extent of the edge.

C. Tunneling through stable gaps

We have demonstrated that turbulent fluctuations can leak or spill into stable regions. This suggests that they can also tunnel through locally stable regions of finite width (i.e., "gaps" in the growth rate profile). The tunneling problem is demonstrated in Fig. 7. We considered tunneling through both marginally stable and heavily damped ($\gamma_d \geqslant \gamma_g$) regions. Such gaps might correspond to small local transport barriers, where $\gamma(x)<0$, which form on account of pressure gradient steepening, mean electric field shear, islands, etc. The prediction of exponential decay for a marginal region with $\gamma=0$ [i.e., Eq. (27b)] indicates that the turbulence can *eventually* tunnel through marginally stable gaps of *all sizes*. Of course, it will take a very long time to tunnel through larger gaps. A simple but interesting plot of gap width versus tunneling time is given in Fig. 8. This plot indicates that the expansion of turbulence into the linearly stable region (with nonlinear damping) proceeds in time as $x \sim t^n$ with $n \sim 1/4$–$1/5$. Finally, a complete analysis of propagating front

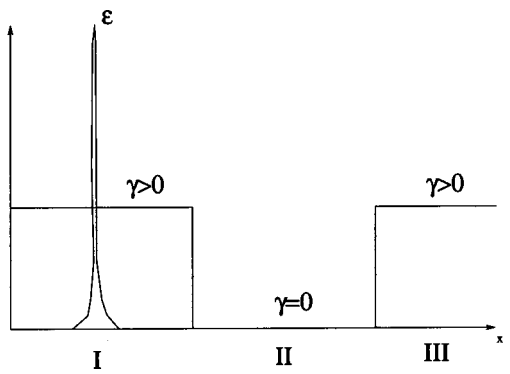

FIG. 7. A sketch of the turbulence tunneling problem. "Tunneling" is said to have occurred when turbulence is observed in the third region.

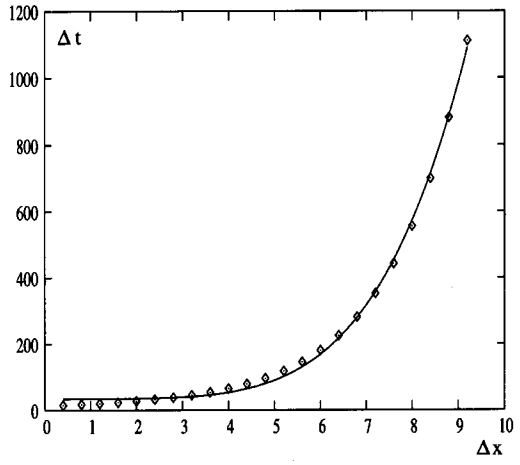

FIG. 8. Turbulence tunneling time vs width of the stable region. The initial time offset is the time elapsed before the turbulence spreads to the edge of the gap. The solid line is a power law fit to an expression of the form $\Delta x/(\Delta t)^n$. Here Δx is normalized to $\lambda=\sqrt{(2D_0/\gamma_{\mathrm{NL}})}$ and time is normalized to the linear growth rate γ.

position versus time for various $\gamma(x)$ profiles can be found in Fig. 9. Figure 9 systematically compares turbulence spreading, first without nonlinear damping [Fig. 9(a)], then with nonlinear damping [Fig. 9(b)]. Note that in the absence of local nonlinear damping, the front position extends without limit exponentially. Even case (c), which has a substantial region with $\gamma<0$ shows no tendency of saturation. On the other hand, with nonlinear damping [Fig. 9(b)], spreading can saturate, depending on the profile of $\gamma(x)$. In particular, case (c) now saturates. The mechanism of this saturation is nonlinear coupling of the stable ($\gamma<0$) and unstable ($\gamma>0$) regions mediated by spreading. Note also that, even with nonlinear damping, the turbulence can jump gaps in $\gamma(x)$, as in case (g), for example. Notice that for case (f), since the particular gap size is larger than the turbulence penetration depth, tunneling does not occur, however for smaller gaps, the same dynamics results in tunneling for that case as well.

IV. DISCUSSION AND CONCLUSIONS

In this paper, we have studied the dynamics of turbulence spreading and nonlocal phenomena in magnetically confined plasmas. The principal results of this investigation are listed below.

(1) A model for the local turbulence intensity evolution was derived using Fokker–Planck theory. The model is further elucidated by comparison and contrast with wave kinetics and with $K-\epsilon$ type turbulence closures. The model involves local growth $[\gamma(x)]$, local nonlinear damping $[\gamma_{\mathrm{NL}}(x)\varepsilon^{\alpha+1}]$ nonlinear diffusion ($D_\varepsilon=D_0\varepsilon^\alpha$), and radial group propagation as a mock-up of toroidicity effects.

(2) The simple model has been extensively explored, using combined analytical and numerical calculations. For the case $\gamma=\gamma_{\mathrm{NL}}=0$, a well-known self-similar solution indicating subdiffusive spreading is recovered. More interestingly for constants γ, γ_{NL}, and D_0, the model reduces to a variant of the familiar Fisher-KPP equation. A ballistically propagating front solution, with $V=(\gamma^2 D_0/2\gamma_{\mathrm{NL}})^{1/2}$, is shown to emerge from the asymptotic limit of a similarity solution. The solution is consistent with the behavior of the well-known leading edge behavior of Fisher fronts.

(3) The penetration of a stable region has been studied. In particular, the depth of penetration into a marginal region as a function of time has been determined, and the penetration depth into a damped region has been calculated. In particular, significant turbulence penetration from a strongly turbulent edge into a marginally stable core is shown to be possible. Several studies of the interaction of a propagating front with a stable "gap" region [i.e., where $\gamma(x)\leqslant 0$] have been completed. Results indicate that turbulence can jump through modest gaps on dynamically interesting scales.

These results have many implications of interest in the context of confinement physics. These implications are as follows.

(1) The time-honored local saturation paradigm (i.e., $\gamma/k_\perp^2=D$) is clearly inadequate and incomplete. A finite initial pulse of turbulence spreads on dynamically interesting time scales, and more rapidly than rates predicted by considerations of transport, alone. For example, the predicted intensity velocity is the geometric mean of the local growth rate and the turbulent diffusivity. Efforts at modeling based on the local saturation paradigm should be reconsidered.

(2) Ballistic fluctuation energy front propagation is possible via dynamics alone, and does not require toroidicity-induced coupling, zonal-flow induced side-band coupling, and other intricate effects. Such front propagation may break gyro-Bohm scaling.

(3) Since turbulence propagation fronts can jump modest gaps in the local growth rate profile, the width of a transport barrier probably must exceed a certain minimum in order for a barrier to be identifiable. Additional physics in the model may be necessary to define a barrier, as well. In particular, modest regions of linear stability may not correspond to the locations of barriers, and the linear growth rate may not be a good indicator of a barrier.

(4) Since turbulence can tunnel into marginal or stable regions, fluctuation energy originating at the strongly turbulent edge may spread into the marginal core relatively easily, thus producing an intermediate region of strong turbulence. This phenomenon blurs the traditionally assumed distinction between the core and edge, and suggests that the boundary between the two is particularly obscure in L mode. It also identifies one element of the global profile readjustment which follows the L→H transition, namely, the quenching of turbulence in the core which originated at the edge.

(5) Tunneling can also allow turbulence to penetrate the "buffer layers" usually setup at the boundaries of numerical simulation domains. Note that should the simulation run time exceed the buffer layer penetration time,

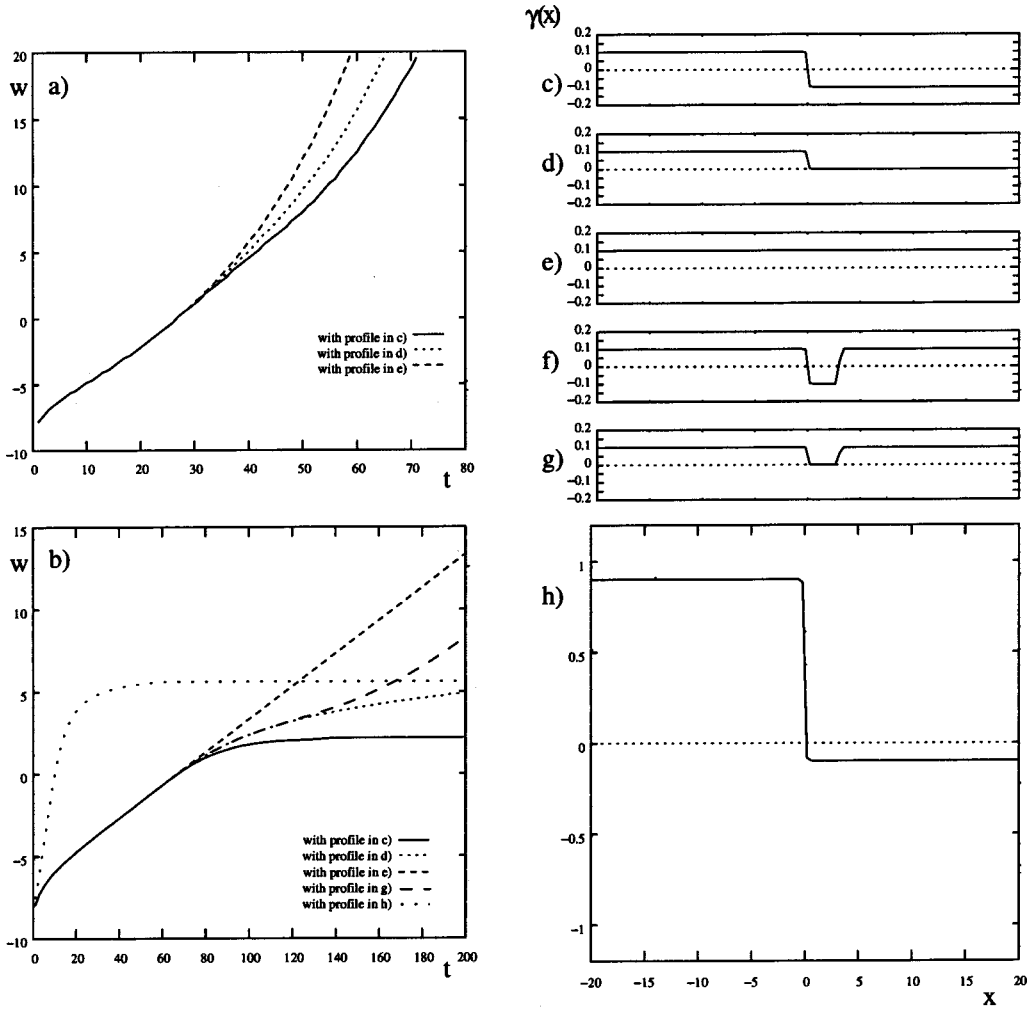

FIG. 9. The front position vs time for various steplike $\gamma(x)$ profiles (a) with $\gamma_{NL}=0$ (i.e., locally unsaturated turbulence), (b) $\gamma_{NL}=1$ (i.e., locally saturated turbulence). Notice that in (b), $\gamma(x)$ profile of (f) gives exactly the same result as the profile of (c), since the steady state turbulence skin depth is less than the gap size for this particular gap size. In particular in part (a) it is clearly seen that if there is no saturation, the spreading is exponential, even when the turbulence is strongly damped in one region [i.e., as in profile (c)]. Part (b), on the other hand, demonstrates the phenomena of reaching steady state [i.e., for profiles (c) and (h)], constant velocity front propagation [i.e., for profile (e)], tunneling through barriers and later assuming the same speed [i.e., for profile (g)], and finally a constant speed spreading followed by a decelerating phase in the marginally stable region for profile (d).

unphysical backscatter of energy from the boundary may occur. Thus, spreading phenomena may limit the time of validity of numerical simulations.

We identify and discuss two extensions of the basic theory. These will be addressed in detail in future publications. First, we consider the role of toroidicity and its consequent induced coupling of poloidal harmonics on turbulence energy propagation. This can be approached by retaining a radial group velocity[12] term in the energy equation (as done here) or, more appropriately, by considering a lattice of coupled poloidal harmonics and the energy transfer between them. The latter corresponds to a study of ballooning effects in real space. This may be facilitated by working in a basis of modelets, as recently discussed by Connor and Hastie.[34] A second issue is the effect of zonal flows (Diamond *et al.*,[35] and references therein) on the spreading dynamics. By shearing the underlying turbulence, zonal flows can produce regions of steep fluctuation intensity gradient, which in turn drive spreading. A broad region of strong zonal flow excitation would likely *inhibit* turbulence spreading. Indeed, the phenomenon of transport barrier formation is a special case of turbulence spreading (i.e., turbulence retreat). The inhibition of turbulence spreading by means of shear layers has been predicted by, and observed in, several models of fluctuation energy and mean flow evolution. Alternatively moderate zonal flow coupling might *enhance* spreading via spatial sideband coupling, as recently advocated by other authors.[20] We thus note that the effects of zonal flows on turbulence energy evolution are numerous, and likely to vary for different regimes of zonal flow damping, turbulence excitation, etc. One upshot of this wealth of possibilities is the possibility of alternating domains consisting predominantly of turbulence and zonal flows, respectively. Such domain wave patterns can propagate through the system.[36,37] This phenomenon of *corrugated spreading* has been observed in gyrokinetic simulations and in numerical studies of a K-ϵ type model with mean field coupling. Thus, spreading may be either smooth or structured and corrugated. At present,

there is no clue as to how the system selects its pattern structure from between these two possibilities.

A second possible extension concerns the validity of the Fokker–Planck theory. It is well known that the Fokker–Planck equation provides a means to compute the time evolution of the probability distribution function for a stochastic system, given the input of the "microscopic" (i.e., single step) transition probability. The latter must be normalizable and must have a finite second moment for the Fokker–Planck approach to be valid. It is by no means clear that the local transition probability for turbulent spreading will *actually* have a convergent second moment. Indeed, since spatial spreading and spectral transfer in wave number space are strongly coupled, it is quite possible that since the wave number spectrum follows a power law, so does the distribution of spatial steps. For self-similar processes described by a power law, this requirement imposes severe constraints on the spectrum.[26] Violation of the condition of a convergent second moment suggests that a nondiffusive Levy process underlies the spreading phenomenon. We speculate here that the divergence of the second moment in the Fokker–Planck theory would also signify a breakdown in weak turbulence theory as the latter is also based upon the assumption of a quasi-Gaussian pdf.[38] A well-known example of such a nondiffusive spreading is the Richardson dispersion law, which predicts that ℓ, the separation between two points in a turbulent flow grows as $\ell^2 \sim \epsilon t^3$. This possibility will be investigated in a future publication.

Another point is that although we used convenient Heaviside step functions for growth rate profiles, in the study of tunneling problem, in fact the basic model [i.e., Eq. (18)] assumes $\gamma(x)$ to be nonzero, continuous, and differentiable. For a turbulent diffusivity derived rigorously from the basic equations it is easily seen that D_ε is tied to γ, via the scaling of the saturated intensity with drive. Alternatively put, there is a time lag (related to the cross phase) between fluctuations and nonlinear interaction. Thus, the above model is not accurate when $\gamma \leqslant 0$. To take this case into account, one needs a minimum of a two-field model. We will consider the simplest possible case, which in practice introduces a time delay between growth and fluctuation-driven radial transport, and this treats the transport as "accumulative." Such a delay is clearly present in the basic theory. The two-field model is

$$\frac{\partial}{\partial t}\varepsilon(x,t) + v_{gx}(x)\frac{\partial}{\partial x}\varepsilon(x,t) + \beta\frac{\partial}{\partial x}[\varepsilon(x,t)\overline{V}(x,t)] - \gamma(x)\varepsilon(x,t) + \gamma_{NL}(x)\varepsilon(x,t)^2 = 0, \tag{29}$$

$$\frac{\partial}{\partial t}\overline{V}(x,t) + \alpha\frac{\partial}{\partial x}\varepsilon(x,t) = 0. \tag{30}$$

In practice for $\varepsilon \sim e^{\gamma t}$, one can integrate the equation for the mean flow and recover the initial model [i.e., Eq. (21)], with $D_0 = \beta\alpha/\gamma$. For the more general case, a sharp gradient near the edge enhances the outward mean intensity flux simply by acting as a conservative force that accelerates the flux. This in turn advects the turbulence outward, reducing the intensity gradient, but since it is the differential drive that produces the gradient (i.e., existence of drive on one side and nonexistence of it on the other), the latter is immediately restored. Since the gradient is always supplied at the same point by the drive, the mean flow speeds at that point increase without limit, until other effects set in. This is the reason we call this type of transport accumulative. Such effects enhance the turbulence tunneling considerably. Although the existence of first-order spatial derivatives in Eqs. (29) and (30) and the fact that the mean flow grows to such large magnitudes near the boundary layer make the numerical problem somewhat more difficult, a qualitative picture of what happens can be found in Fig. 10.

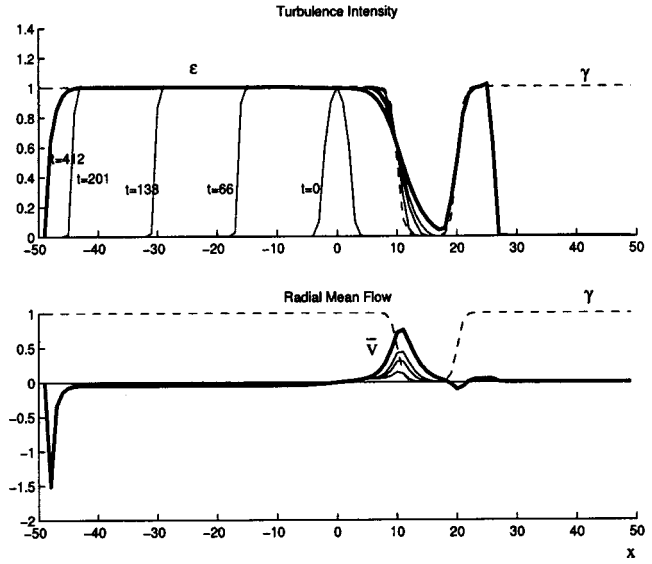

FIG. 10. Turbulence tunneling with the coupled two equation model. Spreading, in the gap region, with this model is observed to be diffusive (i.e., $\Delta x \sim \Delta t^{1/2}$). This could be due to numerical diffusion.

Finally it is worthwhile to discuss the results of this paper on the context of related studies of the theory of turbulence spreading. This discussion is limited to three works, namely, the pioneering study of Garbet *et al.*, in 1994,[12] the recent turbulence model of Chen[20,39] and collaborators, based on zonal flow coupling effects in toroidal geometry, and a new study for the case of subcritical turbulence by Itoh *et al.*, which is otherwise similar to this paper. Simply put, the paper by Garbet *et al.* uses a fluid drift wave model and neglects zonal flows. It predicts diffusive spreading (i.e., $\Delta x^2 \sim t$) for weak turbulence in a cylinder, ballistic spreading (i.e., $\Delta x \sim t$) for weak turbulence in a torus, and an intermediate scaling for strong turbulence, in both cylinder and torus. In contrast, we predict that ballistic spreading is possible *without* toroidal coupling effects, for either weak or strong turbulence. The second work does not present a systematic study of spreading dynamics and its parameter dependencies, but the authors have stated that spreading can be "exponentially fast."[40] Here we find that exponentially fast spreading can occur only if local, nonlinear saturation is neglected. This limit appears questionable, in that it only seems possible to define spreading meaningfully relative to a quasisteady state, which is locally saturated. This model of Chen *et al.* cannot treat strong turbulence, and leaves the important (indeed, crucial for their case) issue of the effect of zonal

flow damping on spreading dynamics unaddressed. If the zonal flow damping is weak, as in the Dimits shift regime, formation of a barrier may be triggered and mean field evolution must be treated as well. At the very least the strong zonal flow shears in the Dimits shift regime should impede spreading by shredding apart extended eddies. On the other hand, if the zonal flow damping is moderate or strong, zonal flow excitation is minimal, so the effect of zonal shears on spreading is likely to be weak. The recent work of Itoh *et al.*[41] predicts that ballistic spreading is possible for subcritical turbulence, provided the size of the initial patch of turbulence exceeds a minimum scale size. In that case also, ballistic expansion of a turbulence intensity front appears in the context of a simple model. It seems as though substantial further research will be necessary in order to resolve the many questions which persist in the theory of turbulence spreading.

ACKNOWLEDGMENTS

The authors would like to thank K. Itoh and S.I. Itoh for stimulating discussions and for their collaboration on related work. They also acknowledge valuable discussions with M. Malkov, L. Villard, X. Garbet, R. Goldston, and W. M. Nevins.

This research was supported by U.S. Department of Energy Grant No. FG02-04ER 54738 (UCSD), Contract No. DE-AC02-76-CHO-3073 (PPPL), and Grant No. DE-FC02-04ER54796 (UCI). P.D. also acknowledges support from the Isaac Newton Istitute, University of Cambridge, where part of this work was completed.

APPENDIX: A BIVARIATE DIFFUSION EQUATION

The wave kinetic equation describes the adiabatic evolution of fluctuation "number" [i.e., quanta density $N(\underline{k},\underline{x},t)$, which is usually, but not always, the wave action density] by a "slow" straining flow. Thus, the wave kinetic equation is a natural description for the evolution of smaller scale waves and turbulence in the presence of comparatively larger, slower (i.e., integral scale) flows. The wave kinetic equation gives

$$\frac{\partial}{\partial t}N + \underline{v}_g \cdot \underline{\nabla} N + \underline{V} \cdot \underline{\nabla} N - \frac{\partial}{\partial \underline{x}}(\underline{k} \cdot \underline{V}) \cdot \frac{dN}{d\underline{k}} = C(N), \quad \text{(A1a)}$$

where

$$\frac{d\underline{k}}{dt} = -\underline{\nabla}(\underline{k} \cdot \underline{V} + \tilde{v}_x \underline{x}). \quad \text{(A1b)}$$

We will hereafter neglect mean flows ($\langle V \rangle \equiv 0$) and focus on the effects of fluctuating flows. Averaging then yields

$$\frac{\partial}{\partial t}\langle N \rangle + v_{gx}\frac{\partial}{\partial t}\langle N \rangle + \partial_x \Gamma_x + \partial_k \Gamma_{k\theta} = \langle C(N) \rangle. \quad \text{(A1c)}$$

Here,

$$\Gamma_x \equiv \langle \tilde{v}_x \tilde{N} \rangle \quad \text{(A2a)}$$

and

$$\Gamma_k = \left\langle -\frac{\partial}{\partial x}(k_r \tilde{v}_x)\tilde{N} \right\rangle \quad \text{(A2b)}$$

define the strain-induced fluxes in space and wave-number space. Application of either quasilinear theory or standard Fokker–Planck methods then yields a bivariate diffusion equation for the mean $\langle N \rangle$, namely,

$$\frac{\partial \langle N \rangle}{\partial t} + v_{gx}\frac{\partial}{\partial x}\langle N \rangle - \frac{\partial}{\partial k_\theta}D_k \frac{\partial \langle N \rangle}{\partial k_\theta} - \frac{\partial}{\partial x}D_x \frac{\partial \langle N \rangle}{\partial x} = \langle C(N) \rangle, \quad \text{(A3a)}$$

where

$$D_k = \sum_q q_\theta^2 k_x^2 |\tilde{v}_q|^2 \Re e[R(\underline{k},\underline{q})], \quad \text{(A3b)}$$

$$D_x = \sum_q |\tilde{v}_q|^2 \Re e[R(\underline{k},\underline{q})], \quad \text{(A3c)}$$

$$R(k,q) = i/\{[\Omega_q - q v_g(k)] + i\Delta\Omega_q\}, \quad \text{(A3d)}$$

are k_θ and spatial diffusion coefficients, respectively, induced by the spectrum of radial flow fluctuations $\langle \tilde{v}^2 \rangle_q$. D_k accounts for refraction to higher k_θ by flow straining and D_x accounts for spatial scattering, caused by the same flow spectrum. $R(\underline{k},\underline{q})$ is the response function which sets the effective correlation time for interaction of wave packets ($\underline{k}$) with the strain field $\tilde{v}_q$. For symmetric spectra, cross-diffusion terms are negligible. Equation (A3a) unambiguously shows that spatial scattering of fluctuation energy, which leads to turbulence spreading, is directly linked to large-scale straining, which also initiates the turbulent cascade. This is a further indication that turbulent spreading is a direct consequence of nonlinear interaction in an inhomogeneous medium. Finally, as large-scale flows are in turn driven by smaller scale stresses, $|\tilde{v}_q|^2$ may be regarded as a functional of N, via a feedback relation of the form

$$\left(\frac{\partial}{\partial t} + \mu\right)\tilde{V}_q = f(q)\sum_{\underline{k}} g(\underline{k})\tilde{N}_q(\underline{k}). \quad \text{(A4)}$$

Here the $g(k)$ is a generic coupling coefficient and $f(q)$ is the inverse of the large-scale dispersion, μ is the decay/growth rate. Thus, the $\langle N \rangle$ equation is seen to be nonlinear in N, as shown in the earlier Fokker–Planck derivation. Finally, we remark that joint reflection symmetry considerations may be used to derive a bivariate Burgers' equation for pulses of wave population density. These pulses may be thought of as avalanches in (x,k_θ) space. This theory is elaborated in Refs. 18 and 22.

[1] P. H. Diamond and T. S. Hahm, Phys. Plasmas **2**, 3640 (1995).
[2] S. I. Itoh and K. Itoh, Plasma Phys. Controlled Fusion **43**, 1055 (2001).
[3] S. I. Itoh and K. Itoh, Phys. Rev. Lett. **60**, 2276 (1988).
[4] F. L. Hinton, Phys. Fluids B **3**, 696 (1991).
[5] D. E. Newman, B. A. Carreras, P. H. Diamond, and T. S. Hahm, Phys. Plasmas **3**, 1858 (1996).
[6] E. J. Synakowski, S. H. Batha, M. A. Beer *et al.*, Phys. Plasmas **4**, 1736 (1997).
[7] K. H. Burrell, E. J. Doyle, P. Gohil *et al.*, Phys. Plasmas **1**, 1536 (1994).
[8] P. H. Diamond, V. B. Lebedev, D. E. Newman, and B. A. Carreras, Phys. Plasmas **2**, 3685 (1995).

[9]B. B. Kadomtsev, *Plasma Turbulence* (Academic, New York, 1965).
[10]G. Barenblatt, *Scaling, Self-similarity, and Intermediate Asymptotics* (Cambridge University Press, Cambridge, 1996).
[11]L. Y. Chen and N. Goldenfeld, Phys. Rev. A **45**, 5572 (1992).
[12]X. Garbet, L. Laurent, A. Samain, and J. Chinardet, Nucl. Fusion **34**, 963 (1994).
[13]R. D. Sydora, V. K. Decyk, and J. M. Dawson, Plasma Phys. Controlled Fusion **38**, A281 (1996).
[14]S. E. Parker, H. E. Mynick, and M. Artun *et al.*, Phys. Plasmas **3**, 1959 (1996).
[15]Z. Lin, S. Ethier, T. S. Hahm, W. W. Lee, J. Lewandowski, G. Revoldt, W. M. Tang, and W. X. Tang, *Proceedings of the Nineteenth International Conference on Plasma Physics and Controlled Nuclear Fusion Research, Lyon, France, 2002* (International Atomic Energy Agency, Vienna, Austria, 2002).
[16]Z. Lin, T. S. Hahm, S. Ethier, and W. M. Tang, Phys. Rev. Lett. **88**, 195004 (2002).
[17]Z. Lin and T. S. Hahm, Phys. Plasmas **11**, 1099 (2004).
[18]E.-J. Kim, P. K. Diamond, M. Malkov *et al.*, Nucl. Fusion **43**, 961 (2003).
[19]T. S. Hahm, P. H. Diamond, Z. Lin, K. Itoh, and S.-I. Itoh, Plasma Phys. Controlled Fusion **46**, A323 (2004).
[20]L. Chen, R. B. White, and F. Zonca, Phys. Rev. Lett. **92**, 075004 (2004).
[21]W. M. Nevins (private communication).
[22]P. H. Diamond and M. Malkov, Phys. Scr., T, **T98**, 63 (2002).
[23]S. Chandrasekhar, Rev. Mod. Phys. **15**, 1 (1943).
[24]M. N. Rosenbluth and C. S. Liu, Phys. Fluids **19**, 815 (1976).
[25]A. Yoshizawa, S.-I. Itoh, K. Itoh, and N. Yokoi, Plasma Phys. Controlled Fusion **43**, R1 (2001).
[26]G. M. Zaslavsky, Phys. Rep. **371**, 461 (2002).
[27]N. G. van Kampen, *Stochastic Processes in Physics and Chemistry* (North-Holland, Amsterdam, 1981).
[28]S. B. Pope, *Turbulent Flows* (Cambridge University Press, Cambridge, 2000).
[29]L. D. Landau and E. M. Lifshitz, *Fluid Mechanics* (Addison-Wesley, Reading, MA, 1959).
[30]R. A. Fisher, Ann. Eugenics **38**, 353 (1937).
[31]A. Kolmogoroff, I. Petrovsky, and N. Piscounoff, Clin. Cancer Res. **1**, 1 (1937).
[32]J. D. Murray, *Mathematical Biology*, 2nd ed. (Springer, Berlin, 1993).
[33]B. B. Kadomtsev (private communication).
[34]J. W. Connor and R. J. Hastie, Phys. Plasmas **11**, 1520 (2004).
[35]P. H. Diamond, S.-I. Itoh, K. Itoh, and T. S. Hahm, Plasma Phys. Control. Fusion (to be published).
[36]L. Villard, S. J. Allfrey, A. Bottino *et al.*, Nucl. Fusion **44**, 172 (2004).
[37]D. del Castillo-Negrete, B. A. Carreras, and V. E. Lynch, Phys. Plasmas **11**, 3854 (2004).
[38]R. Kraichnan, J. Fluid Mech. **5**, 497 (1959).
[39]F. Zonca, R. B. White, and L. Chen, Phys. Plasmas **11**, 2488 (2004).
[40]F. Zonca, R. White, and L. Chen, *Proceedings of Non-linear Paradigm for Drift Wave—Zonal Flow Interplay. Coherence, Chaos and Turbulence, APS-DPP Meeting, Albuquerque, NM, 2003.*
[41]K. Itoh *et al.*, J. Phys. Soc. Jpn. (submitted).